On triply coupled vibrations of axially loaded thin-walled composite beams

Thuc Phuong Vo,* Jaehong Lee,† and Kihak Lee‡

Department of Architectural Engineering, Sejong University
98 Kunja Dong, Kwangjin Ku, Seoul 143-747, Korea.

(Dated: August 20, 2009)

Free vibration of axially loaded thin-walled composite beams with arbitrary lay-ups is presented. This model is based on the classical lamination theory, and accounts for all the structural coupling coming from material anisotropy. Equations of motion for flexural-torsional coupled vibration are derived from the Hamilton's principle. The resulting coupling is referred to as triply coupled vibrations. A displacement-based one-dimensional finite element model is developed to solve the problem. Numerical results are obtained for thin-walled composite beams to investigate the effects of axial force, fiber orientation and modulus ratio on the natural frequencies, load-frequency interaction curves and corresponding vibration mode shapes.

Keywords: Thin-walled composite beam; classical lamination theory; triply coupled vibrations; axial force

I. INTRODUCTION

Fiber-reinforced composite materials have been used over the past few decades in a variety of structures. Composites have many desirable characteristics, such as high ratio of stiffness and strength to weight, corrosion resistance and magnetic transparency. Thin-walled structural shapes made up of composite materials, which are usually produced by pultrusion, are being increasingly used in many engineering fields. However, the structural behavior is very complex due to coupling effects as well as warping-torsion and therefore, the accurate prediction of stability limit state and dynamic characteristics is of the fundamental importance in the design of composite structures.

*Graduate student

†Professor, corresponding author. Tel.:+82-2-3408-3287; fax:+82-2-3408-3331

; Electronic address: jhlee@sejong.ac.kr

‡Associate Professor

The theory of thin-walled members made of isotropic materials was first developed by Vlasov [1] and Gjelsvik [2]. Up to the present, investigation into the stability and vibrational behavior of these members has received widespread attention and has been carried out extensively. Closed-form solution for the flexural and torsional natural frequencies, critical buckling loads of isotropic thin-walled bars are found in the literature (Timoshenko [3,4] and Trahair [5]). For some practical applications, earlier studies have shown that the effect of axial force on the natural frequencies and mode shapes is more pronounced than those of the shear deformation and rotary inertia. Many numerical techniques have been used to solve the dynamic analysis of thin-walled members. One of the most effective approach is to derive the exact stiffness matrices based on the solution of the governing differential equations of motion. Most of those studies adopted an analytical method that required explicit expressions of exact displacement functions for governing equations. Although a large number of studies have been performed on the dynamic characteristics of axially loaded isotropic thin-walled beams [6-9], it should be noted that by using this method there appear some works reported on the free vibration of axially loaded thin-walled closed-section composite beams (Banerjee et al. [10-12], Li et al.[13,14] and Kaya and Ozgumus [15]). For thin-walled open-section composite beams, the works of Kim et al.[16-18] deserved special attention because they evaluated not only the exact element stiffness matrix but also dynamic stiffness matrix to perform the spatially coupled stability and vibration analysis of thin-walled composite I-beam with arbitrary laminations. By using finite element method, Bank and Kao [19] analyzed free and forced vibration of thin-walled composite beams. Cortinez, Machado and Piovan [20,21] presented a theoretical model for the dynamic analysis of thin-walled composite beams with initial stresses. Machado et al. [22] determined the regions of dynamic instability of a simply supported thin-walled composite beam under an axial excitation. The analysis was based on a small strain and moderate rotation theory, which was formulated through the adoption of a second-order displacement field. In their research [20-22], thin-walled composite beams for both open and closed cross-sections and the shear flexibility (bending, non-uniform warping) were incorporated. However, it was strictly valid for symmetric balanced laminates and especially orthotropic laminates. By using using a boundary element method, Sapountzakis and Tsiatas [23] solved the flexural-torsional buckling and vibration problems of Euler-Bernoulli composite beams with arbitrarily cross section. This method overcame the shortcoming of possible thin tube theory solution, which its utilization had been proven to be prohibitive even in thin-walled homogeneous sections.

In this paper, which is an extension of the authors' previous works [24-27], flexural-torsional coupled vibration of axially loaded thin-walled composite beams with arbitrary lay-ups is presented. This model is based on the classical lamination theory, and accounts for all the structural coupling coming from the material anisotropy. The governing

differential equations of motion are derived from the Hamilton's principle. A displacement-based one-dimensional finite element model is developed to solve the problem. Numerical results are obtained for thin-walled composite beams to investigate the effects of axial force, fiber orientation and modulus ratio on the natural frequencies and load-frequency interaction curves as well as corresponding vibration mode shapes.

II. KINEMATICS

The theoretical developments presented in this paper require two sets of coordinate systems which are mutually interrelated. The first coordinate system is the orthogonal Cartesian coordinate system (x, y, z), for which the x and y axes lie in the plane of the cross section and the z axis parallel to the longitudinal axis of the beam. The second coordinate system is the local plate coordinate (n, s, z) as shown in Fig.1, wherein the n axis is normal to the middle surface of a plate element, the s axis is tangent to the middle surface and is directed along the contour line of the cross section. The (n, s, z) and (x, y, z) coordinate systems are related through an angle of orientation θ. As defined in Fig.1 a point P, called the pole, is placed at an arbitrary point x_p, y_p. A line through P parallel to the z axis is called the pole axis.

To derive the analytical model for a thin-walled composite beam, the following assumptions are made:

1. The contour of the thin wall does not deform in its own plane.
2. The linear shear strain $\bar{\gamma}_{sz}$ of the middle surface is zero in each element.
3. The Kirchhoff-Love assumption in classical plate theory remains valid for laminated composite thin-walled beams.
4. Each laminate is thin and perfectly bonded.
5. Local buckling is not considered.

According to assumption 1, the midsurface displacement components $\bar{u}, \bar{v}$ at a point A in the contour coordinate system can be expressed in terms of a displacements U, V of the pole P in the x, y directions, respectively, and the rotation angle Φ about the pole axis,

$$\bar{u}(s, z) = U(z) \sin\theta(s) - V(z) \cos\theta(s) - \Phi(z) q(s) \tag{1a}$$

$$\bar{v}(s, z) = U(z) \cos\theta(s) + V(z) \sin\theta(s) + \Phi(z) r(s) \tag{1b}$$

These equations apply to the whole contour. The out-of-plane shell displacement $\bar{w}$ can now be found from the assumption 2. For each element of middle surface, the shear strain become

$$\bar{\gamma}_{sz} = \frac{\partial \bar{v}}{\partial z} + \frac{\partial \bar{w}}{\partial s} = 0 \tag{2}$$

After substituting for $\bar{v}$ from Eq.(1) and considering the following geometric relations,

$$dx = ds\cos\theta \tag{3a}$$

$$dy = ds\sin\theta \tag{3b}$$

Eq.(2) can be integrated with respect to s from the origin to an arbitrary point on the contour,

$$\bar{w}(s,z) = W(z) - U'(z)x(s) - V'(z)y(s) - \Phi'(z)\omega(s) \tag{4}$$

where differentiation with respect to the axial coordinate z is denoted by primes ($'$); W represents the average axial displacement of the beam in the z direction; x and y are the coordinates of the contour in the (x, y, z) coordinate system; and ω is the so-called sectorial coordinate or warping function given by

$$\omega(s) = \int_{s_\circ}^{s} r(s)ds \tag{5a}$$

The displacement components u, v, w representing the deformation of any generic point on the profile section are given with respect to the midsurface displacements $\bar{u}, \bar{v}, \bar{w}$ by the assumption 3.

$$u(s,z,n) = \bar{u}(s,z) \tag{6a}$$

$$v(s,z,n) = \bar{v}(s,z) - n\frac{\partial \bar{u}(s,z)}{\partial s} \tag{6b}$$

$$w(s,z,n) = \bar{w}(s,z) - n\frac{\partial \bar{u}(s,z)}{\partial z} \tag{6c}$$

The strains associated with the small-displacement theory of elasticity are given by

$$\epsilon_s = \bar{\epsilon}_s + n\bar{\kappa}_s \tag{7a}$$

$$\epsilon_z = \bar{\epsilon}_z + n\bar{\kappa}_z \tag{7b}$$

$$\gamma_{sz} = \bar{\gamma}_{sz} + n\bar{\kappa}_{sz} \tag{7c}$$

where

$$\bar{\epsilon}_s = \frac{\partial \bar{v}}{\partial s}; \quad \bar{\epsilon}_z = \frac{\partial \bar{w}}{\partial z} \tag{8a}$$

$$\bar{\kappa}_s = -\frac{\partial^2 \bar{u}}{\partial z^2}; \quad \bar{\kappa}_z = -\frac{\partial^2 \bar{u}}{\partial z^2}; \quad \bar{\kappa}_{sz} = -2\frac{\partial^2 \bar{u}}{\partial s \partial z} \tag{8b}$$

All the other strains are identically zero. In Eq.(8), $\bar{\epsilon}_s$ and $\bar{\kappa}_s$ are assumed to be zero. $\bar{\epsilon}_z$, $\bar{\kappa}_z$ and $\bar{\kappa}_{sz}$ are midsurface axial strain and biaxial curvature of the shell, respectively. The above shell strains can be converted to beam strain components by substituting Eqs.(1), (4) and (6) into Eq.(8) as

$$\bar{\epsilon}_z = \epsilon_z^\circ + x\kappa_y + y\kappa_x + \omega\kappa_\omega \tag{9a}$$

$$\bar{\kappa}_z = \kappa_y \sin\theta - \kappa_x \cos\theta - \kappa_\omega q \tag{9b}$$

$$\bar{\kappa}_{sz} = 2\bar{\chi}_{sz} = \kappa_{sz} \tag{9c}$$

where $\epsilon_z^\circ, \kappa_x, \kappa_y, \kappa_\omega$ and κ_{sz} are axial strain, biaxial curvatures in the x and y direction, warping curvature with respect to the shear center, and twisting curvature in the beam, respectively defined as

$$\epsilon_z^\circ = W' \tag{10a}$$

$$\kappa_x = -V'' \tag{10b}$$

$$\kappa_y = -U'' \tag{10c}$$

$$\kappa_\omega = -\Phi'' \tag{10d}$$

$$\kappa_{sz} = 2\Phi' \tag{10e}$$

The resulting strains can be obtained from Eqs.(7) and (9) as

$$\epsilon_z = \epsilon_z^\circ + (x + n\sin\theta)\kappa_y + (y - n\cos\theta)\kappa_x + (\omega - nq)\kappa_\omega \tag{11a}$$

$$\gamma_{sz} = n\kappa_{sz} \tag{11b}$$

III. VARIATIONAL FORMULATION

The total potential energy of the system can be stated, in its buckled shape, as

$$\Pi = \mathcal{U} + \mathcal{V} \tag{12}$$

where $\mathcal{U}$ is the strain energy

$$\mathcal{U} = \frac{1}{2}\int_v (\sigma_z\epsilon_z + \sigma_{sz}\gamma_{sz})dv \tag{13}$$

After substituting Eq.(11) into Eq.(13)

$$\mathcal{U} = \frac{1}{2}\int_v \left\{\sigma_z\left[\epsilon_z^\circ + (x + n\sin\theta)\kappa_y + (y - n\cos\theta)\kappa_x + (\omega - nq)\kappa_\omega\right] + \sigma_{sz}n\kappa_{sz}\right\}dv \tag{14}$$

The variation of strain energy can be stated as

$$\delta\mathcal{U} = \int_0^l (N_z\delta\epsilon_z + M_y\delta\kappa_y + M_x\delta\kappa_x + M_\omega\delta\kappa_\omega + M_t\delta\kappa_{sz})dz \tag{15}$$

where $N_z, M_x, M_y, M_\omega, M_t$ are axial force, bending moments in the x- and y-direction, warping moment (bimoment), and torsional moment with respect to the centroid, respectively, defined by integrating over the cross-sectional area A as

$$N_z = \int_A \sigma_z dsdn \tag{16a}$$

$$M_y = \int_A \sigma_z(x + n\sin\theta)dsdn \tag{16b}$$

$$M_x = \int_A \sigma_z(y - n\cos\theta)dsdn \tag{16c}$$

$$M_\omega = \int_A \sigma_z(\omega - nq)dsdn \tag{16d}$$

$$M_t = \int_A \sigma_{sz}ndsdn \tag{16e}$$

The potential of in-plane loads $\mathcal{V}$ due to transverse deflection

$$\mathcal{V} = \frac{1}{2}\int_v \overline{\sigma}_z^0\Big[(u')^2 + (v')^2\Big]dv \tag{17}$$

where $\overline{\sigma}_z^0$ is the averaged constant in-plane edge axial stress, defined by $\overline{\sigma}_z^0 = P_0/A$. The variation of the potential of in-plane loads at the centroid is expressed by substituting the assumed displacement field into Eq.(17) as

$$\begin{aligned}\delta\mathcal{V} = \int_v \frac{P_0}{A}\Big[&U'\delta U' + V'\delta V' + (q^2 + r^2 + 2rn + n^2)\Phi'\delta\Phi' + (\Phi'\delta U' + U'\delta\Phi')\big[n\cos\theta - (y - y_p)\big] \\ &+ (\Phi'\delta V' + V'\delta\Phi')\big[n\cos\theta + (x - x_p)\big]\Big]dv\end{aligned} \tag{18}$$

The kinetic energy of the system is given by

$$\mathcal{T} = \frac{1}{2}\int_v \rho(\dot{u}^2 + \dot{v}^2 + \dot{w}^2)dv \tag{19}$$

where ρ is a density.

The variation of the kinetic energy is expressed by substituting the assumed displacement field into Eq.(19) as

$$\begin{aligned}\delta\mathcal{T} = \int_v \rho\Big\{&\dot{U}\delta\dot{U} + \dot{V}\delta\dot{V} + \dot{W}\delta\dot{W} + (q^2 + r^2 + 2rn + n^2)\dot{\Phi}\delta\dot{\Phi} + (\dot{\Phi}\delta\dot{U} + \dot{U}\delta\dot{\Phi})\Big[n\cos\theta - (y - y_p)\Big] \\ &+ (\dot{\Phi}\delta\dot{V} + \dot{V}\delta\dot{\Phi})\Big[n\cos\theta + (x - x_p)\Big]\Big\}dv\end{aligned} \tag{20}$$

In order to derive the equations of motion, Hamilton's principle is used

$$\delta\int_{t_1}^{t_2}(\mathcal{T} - \Pi)dt = 0 \tag{21}$$

Substituting Eqs.(15),(18) and (20) into Eq.(21), the following weak statement is obtained

$$\begin{aligned} 0 &= \int_{t_1}^{t_2}\int_0^l \Big\{ m_0\dot{W}\delta\dot{W} + \Big[m_0\dot{U} + (m_c + m_0 y_p)\dot{\Phi}\Big]\delta\dot{U} + \Big[m_0\dot{V} + (m_s - m_0 x_p)\dot{\Phi}\Big]\delta\dot{V} \\ &+ \Big[(m_c + m_0 y_p)\dot{U} + (m_s - m_0 x_p)\dot{V} + (m_p + m_2 + 2m_\omega)\dot{\Phi}\Big]\delta\dot{\Phi} \\ &- P_0\Big[\delta U'(U' + \Phi' y_p) + \delta V'(V' - \Phi' x_p) + \delta\Phi'(\Phi'\frac{I_p}{A} + U' y_p - V' x_p)\Big] \\ &- N_z\delta W' + M_y\delta U'' + M_x\delta V'' + M_\omega\delta\Phi'' - 2M_t\delta\Phi'\Big\} dz dt \end{aligned} \tag{22}$$

The expressions of inertia coefficients for thin-walled composite beams are given in Refs.[25,26].

IV. CONSTITUTIVE EQUATIONS

The constitutive equations of a k^{th} orthotropic lamina in the laminate co-ordinate system of section are given by

$$\begin{Bmatrix} \sigma_z \\ \sigma_{sz} \end{Bmatrix}^k = \begin{bmatrix} \bar{Q}^*_{11} & \bar{Q}^*_{16} \\ \bar{Q}^*_{16} & \bar{Q}^*_{66} \end{bmatrix}^k \begin{Bmatrix} \epsilon_z \\ \gamma_{sz} \end{Bmatrix} \tag{23}$$

where $\bar{Q}^*_{ij}$ are transformed reduced stiffnesses. The transformed reduced stiffnesses can be calculated from the transformed stiffnesses based on the plane stress ($\sigma_s = 0$) and plane strain ($\epsilon_s = 0$) assumption. More detailed explanation can be found in Ref.[28].

The constitutive equations for bar forces and bar strains are obtained by using Eqs.(11), (16) and (23)

$$\begin{Bmatrix} N_z \\ M_y \\ M_x \\ M_\omega \\ M_t \end{Bmatrix} = \begin{bmatrix} E_{11} & E_{12} & E_{13} & E_{14} & E_{15} \\ & E_{22} & E_{23} & E_{24} & E_{25} \\ & & E_{33} & E_{34} & E_{35} \\ & & & E_{44} & E_{45} \\ \text{sym.} & & & & E_{55} \end{bmatrix} \begin{Bmatrix} \epsilon^\circ_z \\ \kappa_y \\ \kappa_x \\ \kappa_\omega \\ \kappa_{sz} \end{Bmatrix} \tag{24}$$

where E_{ij} are stiffnesses of thin-walled composite beams and given in Ref.[27].

V. GOVERNING EQUATIONS OF MOTION

The governing equations of motion of the present study can be derived by integrating the derivatives of the varied quantities by parts and collecting the coefficients of of $\delta W, \delta U, \delta V$ and $\delta\Phi$

$$N_z' = m_0\ddot{W} \tag{25a}$$

$$M_y'' + P_0\big(U'' + \Phi'' y_p\big) = m_0\ddot{U} + (m_c + m_0 y_p)\ddot{\Phi} \tag{25b}$$

$$M_x'' + P_0\big(V'' - \Phi'' x_p\big) = m_0\ddot{V} + (m_s - m_0 x_p)\ddot{\Phi} \tag{25c}$$

$$\begin{aligned} M_\omega'' + 2M_t' + P_0\big(\Phi''\frac{I_p}{A} + U'' y_p - V'' x_p\big) &= (m_c + m_0 y_p)\ddot{U} \\ &+ (m_s - m_0 x_p)\ddot{V} + (m_p + m_2 + 2m_\omega)\ddot{\Phi} \end{aligned} \tag{25d}$$

The natural boundary conditions are of the form

$$\delta W : \quad W = W_0 \quad \text{or} \quad N_z = P_0 \tag{26a}$$

$$\delta U : \quad U = U_0 \quad \text{or} \quad M_y' = M_{y_0}' \tag{26b}$$

$$\delta U' : \quad U' = U_0' \quad \text{or} \quad M_y = M_{y_0} \tag{26c}$$

$$\delta V : \quad V = V_0 \quad \text{or} \quad M_x' = M_{x_0}' \tag{26d}$$

$$\delta V' : \quad V' = V_0' \quad \text{or} \quad M_x = M_{x_0} \tag{26e}$$

$$\delta\Phi : \quad \Phi = \Phi_0 \quad \text{or} \quad M_\omega' + 2M_t = M_{\omega_0}' \tag{26f}$$

$$\delta\Phi' : \quad \Phi' = \Phi_0' \quad \text{or} \quad M_\omega = M_{\omega_0} \tag{26g}$$

where the displacements and forces denoted by the subscript zero are prescribed values.

By substituting Eqs.(10) and (24) into Eq.(25), the explicit form of governing equations of motion can be expressed with respect to the laminate stiffnesses E_{ij} as

$$E_{11}W'' - E_{12}U''' - E_{13}V''' - E_{14}\Phi''' + 2E_{15}\Phi'' = m_0\ddot{W} \tag{27a}$$

$$E_{12}W''' - E_{22}U^{iv} - E_{23}V^{iv} - E_{24}\Phi^{iv} + 2E_{25}\Phi''' + P_0(U'' + \Phi'' y_p) = m_0\ddot{U} + (m_c + m_0 y_p)\ddot{\Phi} \tag{27b}$$

$$E_{13}W''' - E_{23}U^{iv} - E_{33}V^{iv} - E_{34}\Phi^{iv} + 2E_{35}\Phi''' + P_0(V'' - \Phi'' x_p) = m_0\ddot{V} + (m_s - m_0 x_p)\ddot{\Phi} \tag{27c}$$

$$\begin{aligned} E_{14}W''' + 2E_{15}W'' - E_{24}U^{iv} - 2E_{25}U''' - E_{34}V^{iv} - 2E_{35}V''' \\ -E_{44}\Phi^{iv} + 4E_{55}\Phi'' + P_0(\Phi''\frac{I_p}{A} + U'' y_p - V'' x_p) &= (m_c + m_0 y_p)\ddot{U} + (m_s - m_0 x_p)\ddot{V} \\ &+ (m_p + m_2 + 2m_\omega)\ddot{\Phi} \end{aligned} \tag{27d}$$

Eq.(27) is most general form for flexural-torsional coupled vibration of axially loaded thin-walled composite beams, and the dependent variables, W, U, V and Φ are fully coupled. If all the coupling effects are neglected and the cross section is symmetrical with respect to both x- and the y-axes, Eq.(27) can be simplified to the uncoupled differential equations as

$$(EA)_{com}W'' = \rho A\ddot{W} \tag{28a}$$

$$-(EI_y)_{com}U^{iv} + P_0U'' = \rho A\ddot{U} \tag{28b}$$

$$-(EI_x)_{com}V^{iv} + P_0V'' = \rho A\ddot{V} \tag{28c}$$

$$-(EI_\omega)_{com}\Phi^{iv} + \Big[(GJ)_{com} + P_0\frac{I_p}{A}\Big]\Phi'' = \rho I_p\ddot{\Phi} \tag{28d}$$

From above equations, $(EA)_{com}$ represents axial rigidity, $(EI_x)_{com}$ and $(EI_y)_{com}$ represent flexural rigidities with respect to x- and y-axis, $(EI_\omega)_{com}$ represents warping rigidity, and $(GJ)_{com}$, represents torsional rigidity of thin-walled composite beams, respectively, written as

$$(EA)_{com} = E_{11} \tag{29a}$$

$$(EI_y)_{com} = E_{22} \tag{29b}$$

$$(EI_x)_{com} = E_{33} \tag{29c}$$

$$(EI_\omega)_{com} = E_{44} \tag{29d}$$

$$(GJ)_{com} = 4E_{55} \tag{29e}$$

It is well known that the three distinct load-frequency interaction curves corresponding to flexural buckling and natural frequencies in the x- and y- direction, and torsional buckling and natural frequency, respectively. They are given by the orthotropy solution for simply supported boundary conditions [29]

$$\omega_{xx_n} = \omega_{x_n}\sqrt{1-\frac{P_0}{P_x}} \tag{30a}$$

$$\omega_{yy_n} = \omega_{y_n}\sqrt{1-\frac{P_0}{P_y}} \tag{30b}$$

$$\omega_{\theta\theta_n} = \omega_{\theta_n}\sqrt{1-\frac{P_0}{P_\theta}} \tag{30c}$$

where $\omega_{x_n}, \omega_{y_n}$ and ω_{θ_n} are corresponding flexural natural frequencies in the x- and y-direction and torsional natural

frequency [4].

$$\omega_{x_n} = \frac{n^2\pi^2}{l^2}\sqrt{\frac{(EI_y)_{com}}{\rho A}} \tag{31a}$$

$$\omega_{y_n} = \frac{n^2\pi^2}{l^2}\sqrt{\frac{(EI_x)_{com}}{\rho A}} \tag{31b}$$

$$\omega_{\theta_n} = \frac{n\pi}{l}\sqrt{\frac{1}{\rho I_p}\Big[\frac{n^2\pi^2}{l^2}(EI_\omega)_{com} + (GJ)_{com}\Big]} \tag{31c}$$

and P_x, P_y and P_θ are also corresponding flexural buckling loads in the x- and y-direction and torsional buckling load [5], respectively.

$$P_x = \frac{\pi^2(EI_y)_{com}}{l^2} \tag{32a}$$

$$P_y = \frac{\pi^2(EI_x)_{com}}{l^2} \tag{32b}$$

$$P_\theta = \frac{A}{I_p}\Big[\frac{\pi^2(EI_\omega)_{com}}{l^2} + (GJ)_{com}\Big] \tag{32c}$$

VI. FINITE ELEMENT FORMULATION

The present theory for thin-walled composite beams described in the previous section was implemented via a displacement based finite element method. The element has seven degrees of freedom at each node, three displacements W, U, V and three rotations U', V', Φ' as well as one warping degree of freedom Φ'. The axial displacement W is interpolated using linear shape functions Ψ_j, whereas the lateral and vertical displacements U, V and axial rotation Φ are interpolated using Hermite-cubic shape functions ψ_j associated with node j and the nodal values, respectively.

$$W = \sum_{j=1}^{2} w_j\Psi_j \tag{33a}$$

$$U = \sum_{j=1}^{4} u_j\psi_j \tag{33b}$$

$$V = \sum_{j=1}^{4} v_j\psi_j \tag{33c}$$

$$\Phi = \sum_{j=1}^{4} \phi_j\psi_j \tag{33d}$$

Substituting these expressions into the weak statement in Eq.(18), the finite element model of a typical element can be expressed as the standard eigenvalue problem

$$([K] - P_0[G] - \omega^2[M])\{\Delta\} = \{0\} \tag{34}$$

where $[K], [G]$ and $[M]$ are the element stiffness matrix, the element geometric stiffness matrix and the element mass matrix, respectively. The explicit forms of $[K], [G]$ and $[M]$ are given in Refs.[24-27].

In Eq.(34), $\{\Delta\}$ is the eigenvector of nodal displacements corresponding to an eigenvalue

$$\{\Delta\} = \{W\ U\ V\ \Phi\}^{\mathrm{T}} \tag{35}$$

VII. NUMERICAL EXAMPLES

For verification purpose, flexural-torsional buckling and vibration analysis of a cantilever isotropic mono-symmetric channel section beam (Fig.2), with length l =2m under an axial force at the centroid is performed. The material properties are assumed to be: $E = 0.3\text{GPa}\ , G = 0.115\text{GPa}\ , \rho = 7850\text{kg/m}^3$. Ten Hermitian beam elements with two nodes are used in the numerical examples. The buckling loads are evaluated and compared with numerical results of Kim et al.[9], which is based on dynamic stiffness formulation and ABAQUS solutions, in Table I. Next, the flexural-torsional coupled vibration analysis of axially loaded cantilever beam is analyzed. The value of 6.995N is adopted as initial compressive and tensile forces, which is the half of the critical buckling load of the beam. The lowest four natural frequencies with and without the axial force are presented in Table II. Tables I and II show that the present results are in a good agreement with those by Kim et al.[9].

The next example demonstrates the accuracy and validity of this study for thin-walled composite beams. The symmetric angle-ply I-beams with various fiber angles and two boundary conditions are considered. Following dimensions for I-beam are used: both of flanges width and web height are 50mm. The flanges and web are assumed to be symmetrically laminated with respect to its midplane and made of sixteen layers with each layer 0.13mm in thickness. All computations are carried out with the following material properties: $E_1 = 53.78\text{GPa}\ , E_2 = 17.93\text{GPa}\ , G_{12} = 8.96\text{GPa}, \nu_{12} = 0.25, \rho = 1968.9\text{kg/m}^3$, where subscripts '1' and '2' correspond to directions parallel and perpendicular to fiber direction, respectively. The critical buckling loads of a cantilever composite I-beam with length l =1m and the first six natural frequencies of a simply supported one with length l =2m are given in Tables III and IV. The present solution again indicates good agreement with the analytical approach by Kim et al.[17,18] and Roberts [30] for all lamination schemes considered. The effect of axial force on the fundamental natural frequency of a cantilever and simply supported beam with various fiber angles is exhibited in Figs.3 and 4. For simply supported boundary condition, when fiber angle is equal to 0°, 30° and 60°, at about P=5.75×10^3N, 3.86×10^3N and 2.11×10^3N, respectively, the fundamental natural frequencies become zero which implies that at these loads, the critical bucklings occur as a degenerate case of natural vibration at zero frequency. Figs.3 and 4 also explain the duality between

flexural-torsional buckling and natural frequency.

A simply supported composite I-beam with length $l = 8$m is considered to investigate the effects of axial force, fiber orientation on the natural frequencies and load-frequency interaction curves as well as corresponding vibration mode shapes. The geometry and stacking sequences of the I-section are shown in Fig.5, and the following engineering constants are used

$$E_1/E_2 = 25, G_{12}/E_2 = 0.6, \nu_{12} = 0.25 \tag{36}$$

For convenience, the following nondimensional axial force and natural frequency are used

$$\overline{P} = \frac{Pl^2}{b_3^3 t E_2} \tag{37}$$

$$\overline{\omega} = \frac{\omega l^2}{b_3}\sqrt{\frac{\rho}{E_2}} \tag{38}$$

The top and bottom flanges are angle-ply laminates $[\theta/-\theta]$, and the web laminates are assumed to be undirectional (Fig.5a). All the coupling stiffnesses are zero, but E_{35} does not vanish due to unsymmetric stacking sequence of the flanges. The lowest three natural frequencies with and without the effect of axial force are given in Table V. The critical buckling loads and the natural frequencies without axial force agree completely with those of previous papers [24,25], as expected. The change in the natural frequencies due to axial force is significant for all fiber angles. It is noticed that the natural frequencies diminish as the axial force changes from tension ($\overline{P} = -0.5P_{cr}$) to compression ($\overline{P} = 0.5P_{cr}$). It reveals that the tension force has a stiffening effect while the compressive force has a softening effect on the natural frequencies. The lowest three load-frequency interaction curves with the fiber angle $\theta = 0^\circ$ and 30° obtained by finite element analysis and the orthotropy solution, which neglects the coupling effects of E_{35} from Eqs.(30a)-(30c), are plotted in Figs.6 and 7. For unidirectional fiber direction, the lowest load-frequency interaction curve exactly corresponds to the first flexural in x-direction and the larger ones correspond to the torsional mode and the second flexural in x-direction of the orthotropy solution, respectively. As the fiber angle increases, the vibration mode 1 and 3 are the first and second flexural mode in x-direction. Thus, the othotropy solution and the finite element analysis are identical. However, the vibration mode 2 exhibits double coupling (the first flexural mode in y-direction and torsional mode). Due to the small coupling stiffnesses E_{35}, this mode becomes predominantly the torsional mode, with a little contribution from flexural mode. Therefore, the results by the finite element analysis ($\omega_2 - P_2$) and orthotropy solution ($\omega_{\theta_1} - P_{\theta_1}$) show slight discrepancy in Fig.7. Characteristic of load-frequency interaction curves is that the value of the axial force for which the natural frequency vanishes constitutes the buckling load. Thus, for $\theta = 30^\circ$, the first flexural buckling in minor axis occurs at $\overline{P} = 1.41$. As a result, the lowest branch vanishes

when $\overline{P}$ is slightly over this value. As the axial force increases, two interaction curves ($\omega_2 - P_2$) and ($\omega_{x_2} - P_{x_2}$) intersect at $\overline{P} = 5.41$, thus, after this value, vibration mode 2 and 3 change each other. Finally, the second, third branch will also disappear when $\overline{P}$ is slightly over 5.65 and 6.37, respectively. A comprehensive three dimensional interaction diagram of the natural frequencies, axial compressive force and fiber angle is plotted in Fig.8. Three groups of curves are observed. The smallest group is for the first flexural mode in x-direction and the larger ones are for the flexural-torsional coupled mode and the second flexural mode in y-direction and, respectively.

The next example is the same as before except that in this case, the bottom flange is angle-ply laminates $[\theta/-\theta]$, while the top flange and web laminates are unidirectional, (Fig.5b). For this lay-up, the coupling stiffnesses E_{15} and E_{35} become no more negligibly small. Major effects of axial force on the natural frequencies are again seen in Table VI. Three dimensional interaction diagram between the flexural-torsional buckling loads and natural frequencies with respect to the fiber angle change in the bottom flange is shown in Fig.9. Similar phenomena as the previous example can be observed except that in this case all three groups of curves are flexural-torsional coupled mode. As fiber angle increases about $\theta = 40^\circ$, two larger groups intersect each other. The lowest three load-frequency interaction curves by the finite element analysis and orthotropy solution with the fiber angle $\theta = 30^\circ$ and 60° are displayed in Figs.10 and 11. It can be remarked again that the natural frequencies decrease with the increase of axial forces, and the decrease becomes more quickly when axial forces are close to buckling loads. Due to strong coupling, the orthotropy solution and the finite element analysis solution show significantly discrepancy. It can be explained partly by the typical normal mode shapes corresponding to the first four natural frequencies with fiber angle $\theta = 30^\circ$ for the case of an axial compressive force ($\overline{P} = 0.5P_{cr}$) in Figs.12-15. Relative measures of flexural displacements and torsional rotation show that all the modes are coupled mode (flexural mode in the x- and y-directions and torsional mode). That is, the orthotropy solution is no longer valid for unsymmetrically laminated beams, and triply flexural-torsional coupled should be considered even for a doubly symmetric cross-section.

Finally, the effects of modulus ratio (E_1/E_2) on the first three natural frequencies of a cantilever composite beam under an axial compressive force and tensile force ($\overline{P} = \pm 0.5\overline{P}_{cr}$) are investigated. The stacking sequence of the flanges and web are $[0/90]_s$, (Fig.5c). For this lay-up, all the coupling stiffnesses vanish and thus, the three distinct vibration mode, flexural vibration in the x- and y-direction and torsional vibration are identified. It is observed from Fig.16 that the natural frequencies $\omega_{xx_1}, \omega_{\theta\theta_1}$ and ω_{xx_2} increase with increasing orthotropy (E_1/E_2) for two cases considered.

VIII. CONCLUDING REMARKS

An analytical model is developed to study the flexural-torsional coupled vibration of thin-walled composite beams with arbitrary lay-ups under a constant axial force. This model is capable of predicting accurately the natural frequencies and load-frequency interaction curves as well as corresponding vibration mode shapes for various configurations. To formulate the problem, a one-dimensional displacement-based finite element method is employed. All of the possible vibration mode shapes including the flexural mode in the x- and y-direction and the torsional mode, and triply coupled flexural-torsional mode are included in the analysis. The present model is found to be appropriate and efficient in analyzing free vibration problem of thin-walled composite beams under a constant axial force.

Acknowledgments

The support of the research reported here by a grant (code #06 R&D B03) from Cutting-edge Urban Development Program funded by the Ministry of Land, Transport and Maritime Affairs of Korea government is gratefully acknowledged. The authors also would like to thank the anonymous reviewers for their suggestions and comments in improving the standard of the manuscript.

References

[1] Vlasov VZ. Thin Walled Elastic Beams, Israel Program for Scientific Translation, Jerusalem, 1961.

[2] Gjelsvik A. The theory of thin-walled bars, New York: John Wiley and Sons Inc., 1981.

[3] Timoshenko SP and Gere JM. Theory of elastic stability. New York: McGraw-Hill, 1961.

[4] Timoshenko SP, Young DH and Weaver W. Vibration problems in engineering. New York: Wiley, 1974.

[5] Trahair NS. Flexural-torsional buckling of structures. London: CRC Press, 1993.

[6] Leung AYT. Dynamic stiffness analysis of thin-walled structures. Thin-Walled Struct 1992; 14(3):209-222.

[7] Leung AYT. Exact dynamic stiffness for axial-torsional buckling of structural frames. Thin-Walled Struct 2008; 46(1):1-10.

[8] Kim MY, Yun HT and Kim NI. Exact dynamic and static element stiffness matrices of nonsymmetric thin-walled beam-columns. Comput Struct 2003; 81(14):1425-1448.

[9] Kim NI, Fu CC and Kim MY. Stiffness matrices for flexural-torsional/lateral buckling and vibration analysis of thin-walled beam. J Sound Vib 2007; 299(4-5):739-756.

[10] Banerjee JR and Williams FW. Exact dynamic stiffness matrix for composite Timoshenko beams with applications. J Sound Vib 1996; 194(4):573-585.

[11] Banerjee JR. Free vibration of axially loaded composite Timoshenko beams using the dynamic stiffness matrix method. Comput Struct 1998;69(2):197-208.

[12] Banerjee JR and Su H. Dynamic stiffness formulation and free vibration analysis of a spinning composite beam. Comput Struct 2006; 84(19-20):1208-1214.

[13] Li J, Shen R and Jin X. Bending-torsional coupled dynamic response of axially loaded composite Timosenko thin-walled beam with closed cross-section. Compos Struct 2004;64(1):23-35.

[14] Li J, Wu G, Shen R and Hua H. Stochastic bending-torsion coupled response of axially loaded slender composite thin-walled beams with closed cross-sections. Int J Mech Sci 2005; 47(1):134-155.

[15] Kaya MO and Ozgumus OO. Flexural-torsional-coupled vibration analysis of axially loaded closed-section composite Timoshenko beam by using DTM. J Sound Vib 2007; 306(3-5):495-506.

[16] Kim NI, Shin DK and Kim MY. Improved flexural-torsional stability analysis of thin-walled composite beam and exact stiffness matrix. Int J Mech Sci 2007; 49(8):950-969.

[17] Kim NI, Shin DK and Kim MY. Flexural-torsional buckling loads for spatially coupled stability analysis of thin-walled composite columns. Adv Eng Softw 2008; 39(12):949-961.

[18] Kim NI, Shin DK and Park YS. Dynamic stiffness matrix of thin-walled composite I-beam with symmetric and arbitrary laminations. J Sound Vib 2008; 318(1-2):364-388.

[19] Bank LC and Kao CH. Dynamic Response of Thin-Walled Composite Material Timoshenko Beams. J Energ Resour 1990; 112(2):149-154.

[20] Cortinez VH and Piovan MT. Vibration and buckling of composite thin-walled beams with shear deformability. J Sound Vib 2002; 258(4-5):701-723.

[21] Machado SP and Cortinez VH. Free vibration of thin-walled composite beams with static initial stresses and deformations. Eng Struct 2007; 29(3):372-382.

[22] Machado SP, Filipich CP and Cortinez VH. Parametric vibration of thin-walled composite beams with shear deformation. J Sound Vib 2007;305(4-5):563-581.

[23] Sapountzakis EJ and Tsiatas GC. Flexural-Torsional Buckling and Vibration Analysis of Composite Beams. Comput Mater Con 2007; 6(2), 103-115.

[24] Lee J and Kim S. Flexural-torsional buckling of thin-walled I-section composites. Comput Struct 2001;79(10):987-995.

[25] Lee J and Kim S. Free vibration of thin-walled composite beams with I-shaped cross-sections. Compos Struct 2002; 55(2):205-215.

[26] Lee J and Kim S. Flexural-torsional coupled vibration of thin-walled composite beams with channel sections. Comput Struct 2002; 80(2):133-144.

[27] Lee J and Lee S. Flexural-torsional behavior of thin-walled composite beams. Thin-Walled Struct 2004; 42(9):1293-1305.

[28] Jones RM. Mechanics of composite materials, New York: Hemisphere Publishing Corp., 1975.

[29] Mohri F, Azrar L and Potier-Ferry M. Vibration analysis of buckled thin-walled beams with open sections. J Sound Vib 2004; 275(1-2):434-446.

[30] Roberts TM. Natural frequencies of thin-walled bars of open cross-section. J Struct Eng 1987; 112(10):1584-1593.

CAPTIONS OF TABLES

Table I: Flexural-torsional bucking loads of a cantilever isotropic mono-symmetric channel section beam (N).

Table II: Effect of axial force on the first four natural frequencies of a cantilever isotropic mono-symmetric channel section beam (rad/s).

Table III: Critical bucking loads (N) of a cantilever composite I-beam with symmetric angle-ply laminates $[\pm\theta]_{4s}$ in the flanges and web.

Table IV: Natural frequencies (Hz) of a simply supported composite I-beam with symmetric angle-ply laminates $[\pm\theta]_{4s}$ in the flanges and web.

Table V: Effect of axial force on the first three natural frequencies of a simply supported composite beam with angle-ply laminates $[\theta/-\theta]$ in the flanges.

Table VI: Effect of axial force on the first three natural frequencies of a simply supported composite beam with angle-ply laminates $[\theta/-\theta]$ in the bottom flange.

CAPTIONS OF FIGURES

Figure 1: Definition of coordinates in thin-walled open sections.

Figure 2: Isotropic mono-symmetric channel section for verification.

Figure 3: Effect of axial force on the fundamental natural frequency with the fiber angle 0°, 30° and 60° in the flanges and web of a simply supported composite beam.

Figure 4: Effect of axial force on the fundamental natural frequency with the fiber angle 0°, 30° and 60° in the flanges and web of a cantilever composite beam.

Figure 5: Geometry and stacking sequences of thin-walled composite I-beam.

Figure 6: Effect of axial force on the first three natural frequencies with the fiber angle 0° in the flanges of a simply supported composite beam.

Figure 7: Effect of axial force on the first three natural frequencies with the fiber angle 30° in the flanges of a simply supported composite beam.

Figure 8: Three dimensional interaction diagram between the axial compressive force and the first three natural frequencies with respect to the fiber angle change in the flanges of a simply supported composite beam.

Figure 9: Three dimensional interaction diagram between the axial compressive force and the first three natural frequencies with respect to the fiber angle change in the bottom flange of a simply supported composite beam.

Figure 10: Effect of axial force on the first three natural frequencies with the fiber angle 30° in the bottom flange of a simply supported composite beam.

Figure 11: Effect of axial force on the first three natural frequencies with the fiber angle 60° in the bottom flange of a simply supported composite beam.

Figure 12: Mode shapes of the flexural and torsional components for the first mode $\omega_1 = 2.615$ with the fiber angle 30° in the bottom flange of a simply supported composite beam under an axial compressive force ($\overline{P} = 0.5\overline{P}_{cr}$).

Figure 13: Mode shapes of the flexural and torsional components for the second mode $\omega_2 = 4.805$ with the fiber angle 30° in the bottom flange of a simply supported composite beam under a axial compressive force ($\overline{P} = 0.5\overline{P}_{cr}$).

Figure 14: Mode shapes of the flexural and torsional components for the third mode $\omega_3 = 12.107$ with the fiber angle 30° in the bottom flange of a simply supported composite beam under an axial compressive force ($\overline{P} = 0.5\overline{P}_{cr}$).

Figure 15: Mode shapes of the flexural and torsional components for the fourth mode $\omega_4 = 16.221$ with the fiber angle 30° in the bottom flange of a simply supported composite beam under an axial compressive force ($\overline{P} = 0.5\overline{P}_{cr}$).

Figure 16: Variation of the first three natural frequencies with respect to modulus ratio change of a cantilever

composite beam under an axial compressive force ($\overline{P} = 0.5\overline{P}_{cr}$) and tensile force ($\overline{P} = -0.5\overline{P}_{cr}$).

TABLE I Flexural-torsional bucking loads of a cantilever isotropic mono-symmetric channel section beam (N).

Mode	Kim et al. [9]		Present
	ABAQUS	Theory	
1	14.001	13.800	13.993
2	113.100	112.550	114.346
3	190.080	191.840	191.956
4	256.670	258.540	263.649

TABLE II Effect of axial force on the first four natural frequencies of a cantilever isotropic mono-symmetric channel section beam (rad/s).

Mode	P=6.995 N (compression)		P=0 (no axial force)		P=-6.995 N (tension)	
	Ref.[9]	Present	Ref.[9]	Present	Ref.[9]	Present
1	0.118	0.108	0.164	0.166	0.197	0.206
2	0.570	0.570	0.580	0.582	0.589	0.593
3	0.825	0.830	0.841	0.849	0.854	0.864
4	1.002	1.003	1.036	1.045	1.072	1.087

TABLE III Critical bucking loads (N) of a cantilever composite I-beam with symmetric angle-ply laminates $[\pm\theta]_{4s}$ in the flanges and web.

Lay-ups	Kim et al. [17]		Present
	ABAQUS	Theory	
$[0]_{16}$	5720.0	5755.2	5741.5
$[15/-15]_{4s}$	5174.0	5199.8	5189.0
$[30/-30]_{4s}$	3848.0	3861.0	3854.5
$[45/-45]_{4s}$	2665.0	2672.7	2668.4
$[60/-60]_{4s}$	2119.0	2114.7	2111.3
$[75/-75]_{4s}$	1950.0	1948.3	1945.1

TABLE IV Natural frequencies (Hz) of a simply supported composite I-beam with symmetric angle-ply laminates $[\pm\theta]_{4s}$ in the flanges and web.

Lay-ups	Formulation	Mode					
		1	2	3	4	5	6
$[0]_{16}$	Ref.[18]	24.194	35.233	45.235	96.726	109.441	180.616
	Ref.[30]	24.198	35.240	45.262	96.792	109.516	181.048
	Present	24.198	35.229	45.262	96.792	109.485	181.048
$[15/-15]_{4s}$	Ref.[18]	22.997	36.247	42.996	91.940	107.655	171.678
	Ref.[30]	23.001	36.253	43.022	92.003	107.729	172.089
	Present	23.001	36.124	43.022	92.003	107.538	172.089
$[30/-30]_{4s}$	Ref.[18]	19.816	37.051	37.864	79.225	102.159	147.938
	Ref.[30]	19.820	37.073	37.871	79.279	102.229	148.291
	Present	19.820	36.848	37.073	79.279	100.710	148.290
$[45/-45]_{4s}$	Ref.[18]	16.487	30.827	37.915	65.916	94.884	123.085
	Ref.[30]	16.490	30.845	37.921	65.961	94.949	123.380
	Present	16.490	30.845	35.171	65.961	90.605	123.379
$[60/-60]_{4s}$	Ref.[18]	14.666	27.420	35.372	58.633	87.051	109.484
	Ref.[30]	14.668	27.437	35.378	58.673	87.111	109.746
	Present	14.668	27.437	32.254	58.673	82.109	109.747
$[75/-75]_{4s}$	Ref.[18]	14.077	26.319	31.313	56.278	79.330	105.087
	Ref.[30]	14.079	26.335	31.318	56.316	79.385	105.339
	Present	14.079	26.335	29.985	56.316	77.289	105.338
$[90/-90]_{4s}$	Ref.[18]	13.970	26.119	29.175	55.850	75.767	104.287
	Ref.[30]	13.972	26.134	29.180	55.880	75.819	104.537
	Present	13.972	26.135	29.172	55.888	75.798	104.538

TABLE V Effect of axial force on the first three natural frequencies of a simply supported composite beam with angle-ply laminates $[\theta/-\theta]$ in the flanges.

Fiber	Buckling	$\overline{P} = 0.5\overline{P}_{cr}$ (compression)			$\overline{P}$=0 (no axial force)			$\overline{P} = -0.5\overline{P}_{cr}$ (tension)		
angle	loads ($\overline{P}_{cr}$)	ω_1	ω_2	ω_3	ω_1	ω_2	ω_3	ω_1	ω_2	ω_3
0	5.153	3.566	5.854	18.869	5.043	6.854	20.148	6.176	7.726	20.461
15	4.029	3.153	5.906	16.683	4.459	6.696	17.835	5.461	7.403	18.514
30	1.414	1.868	5.295	9.883	2.641	5.616	10.565	3.235	5.919	11.206
45	0.465	1.072	4.460	5.671	1.516	4.587	6.062	1.856	4.711	6.430
60	0.268	0.813	3.867	4.300	1.149	3.951	4.597	1.408	4.034	4.876
75	0.226	0.746	3.564	3.949	1.055	3.641	4.222	1.293	3.717	4.478
90	0.218	0.734	3.474	3.885	1.038	3.550	4.153	1.272	3.626	4.405

TABLE VI Effect of axial force on the first three natural frequencies of a simply supported composite beam with angle-ply laminates $[\theta/-\theta]$ in the bottom flange.

Fiber	Buckling	$\overline{P} = 0.5\overline{P}_{cr}$ (compression)			$\overline{P}$=0 (no axial force)			$\overline{P} = -0.5\overline{P}_{cr}$ (tension)		
angle	loads ($\overline{P}_{cr}$)	ω_1	ω_2	ω_3	ω_1	ω_2	ω_3	ω_1	ω_2	ω_3
0	5.153	3.566	5.854	18.869	5.043	6.854	20.148	6.176	7.726	20.461
15	4.565	3.356	5.856	17.703	4.746	6.750	18.919	5.813	7.539	19.493
30	2.771	2.615	4.805	12.107	3.698	5.470	13.183	4.529	6.063	14.175
45	1.631	2.006	4.296	7.362	2.837	4.742	8.384	3.475	5.148	9.294
60	1.259	1.762	4.204	5.824	2.492	4.558	6.808	3.053	4.887	7.666
75	1.140	1.677	4.180	5.399	2.372	4.504	6.356	2.905	4.806	7.187
90	1.112	1.656	4.174	5.311	2.342	4.491	6.259	2.869	4.786	7.082

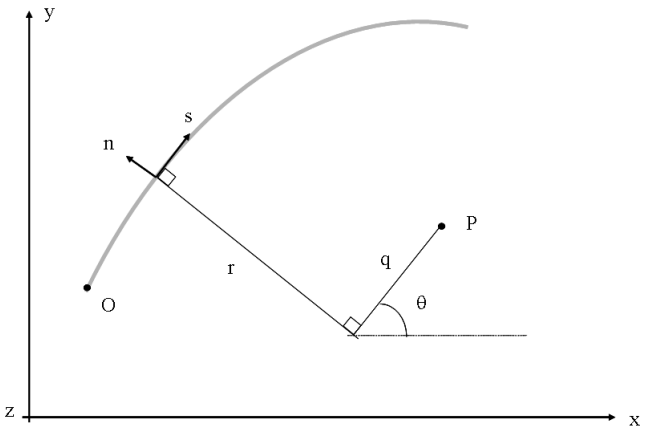

FIG. 1 Definition of coordinates in thin-walled open sections.

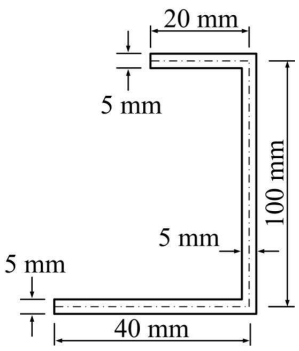

FIG. 2 Isotropic mono-symmetric channel section for verification.

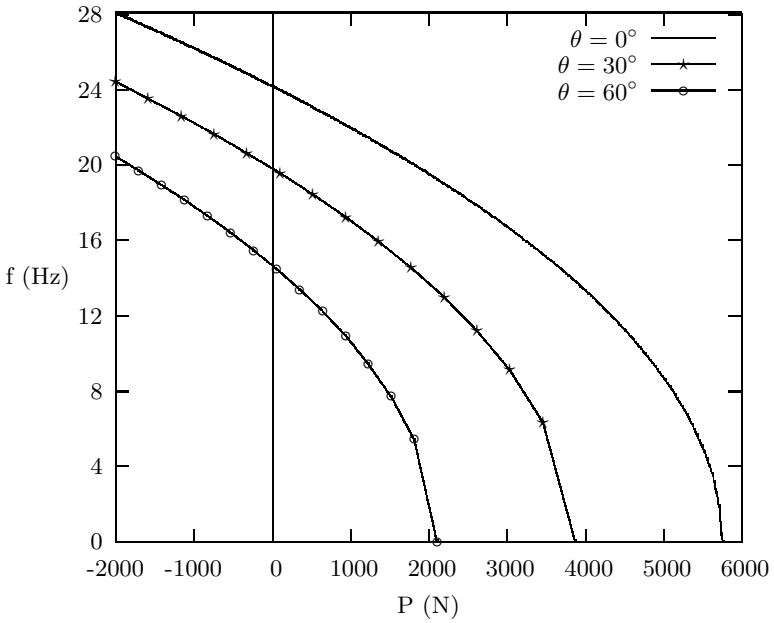

FIG. 3 Effect of axial force on the fundamental natural frequency with the fiber angle 0°, 30° and 60° in the flanges and web of a simply supported composite beam.

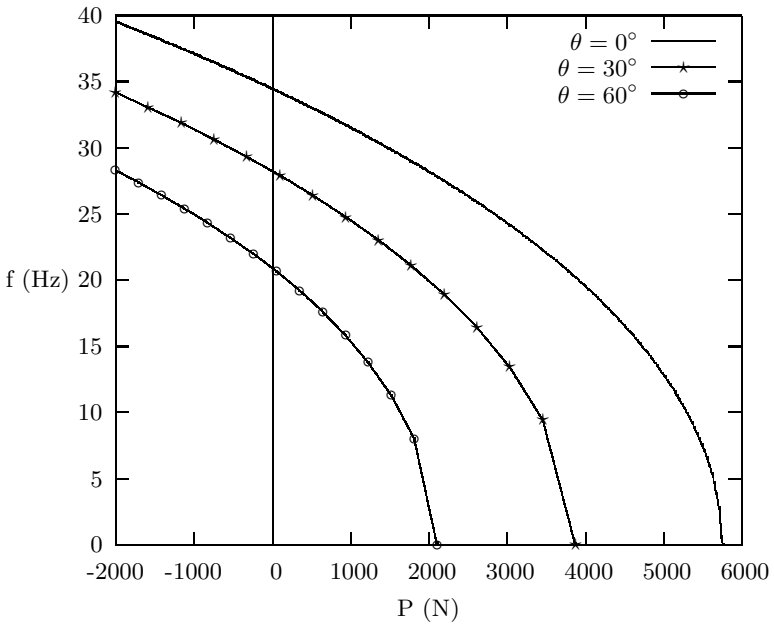

FIG. 4 Effect of axial force on the fundamental natural frequency with the fiber angle 0°, 30° and 60° in the flanges and web of a cantilever composite beam.

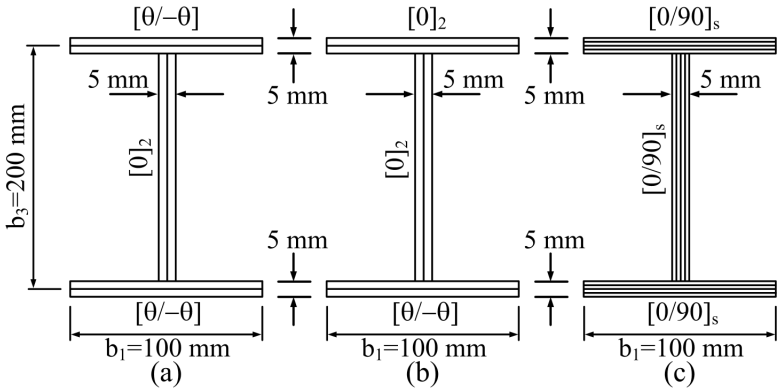

FIG. 5 Geometry and stacking sequences of thin-walled composite I-beam.

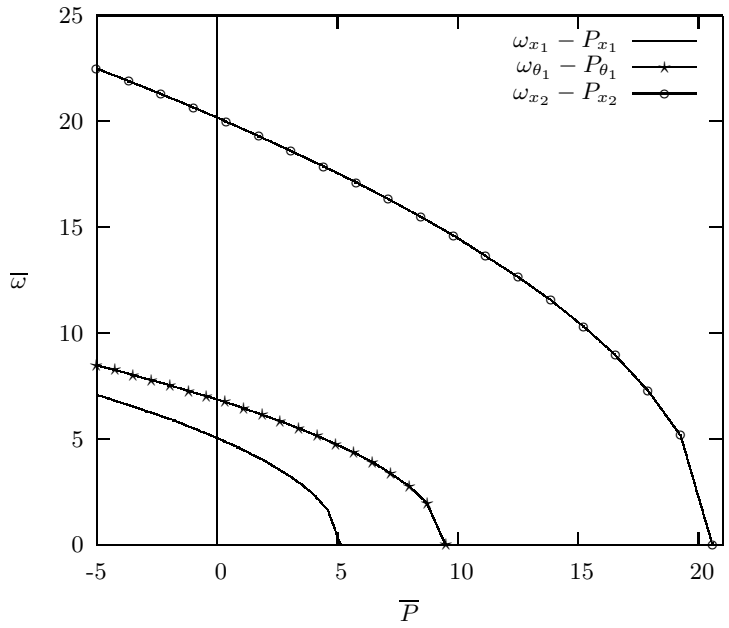

FIG. 6 Effect of axial force on the first three natural frequencies with the fiber angle 0° in the flanges of a simply supported composite beam.

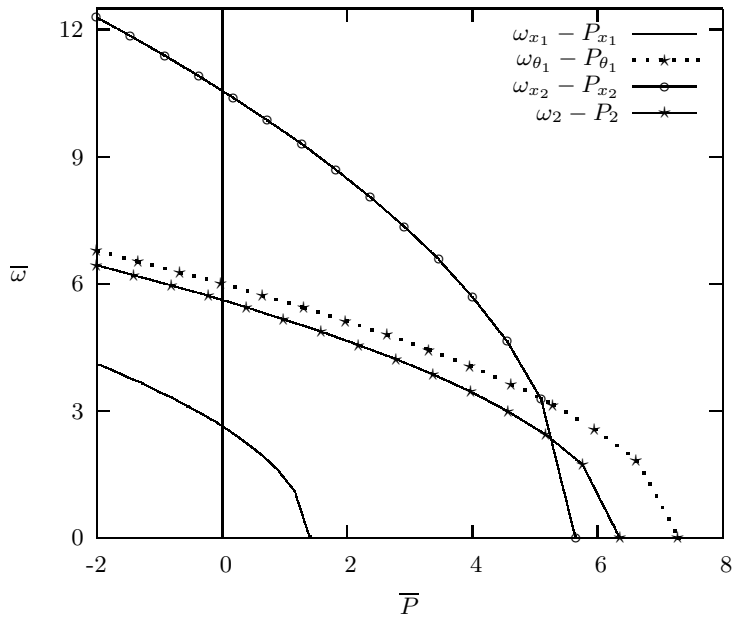

FIG. 7 Effect of axial force on the first three natural frequencies with the fiber angle 30° in the flanges of a simply supported composite beam.

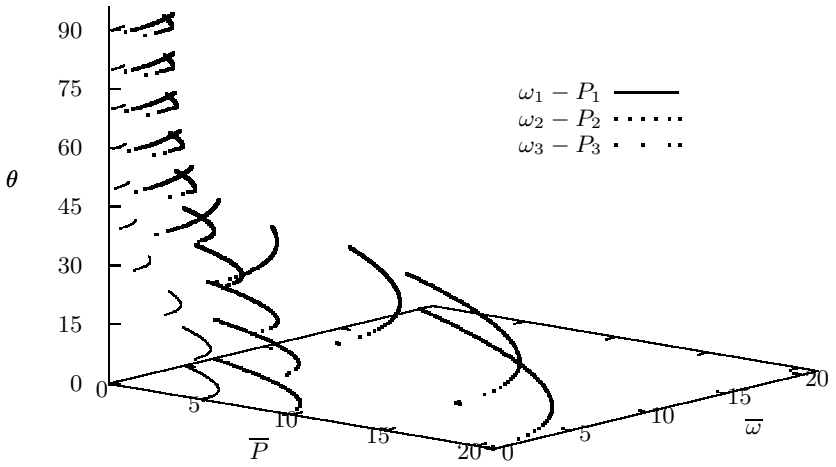

FIG. 8 Three dimensional interaction diagram between the axial compressive force and the first three natural frequencies with respect to the fiber angle change in the flanges of a simply supported composite beam.

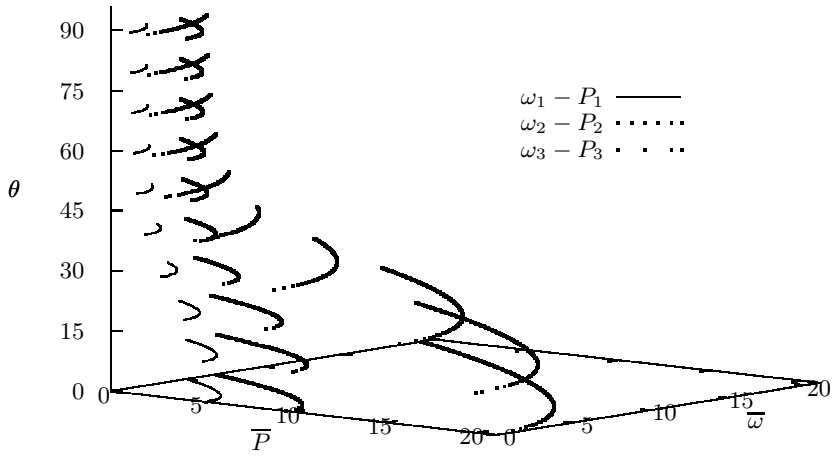

FIG. 9 Three dimensional interaction diagram between the axial compressive force and the first three natural frequencies with respect to the fiber angle change in the bottom flange of a simply supported composite beam.

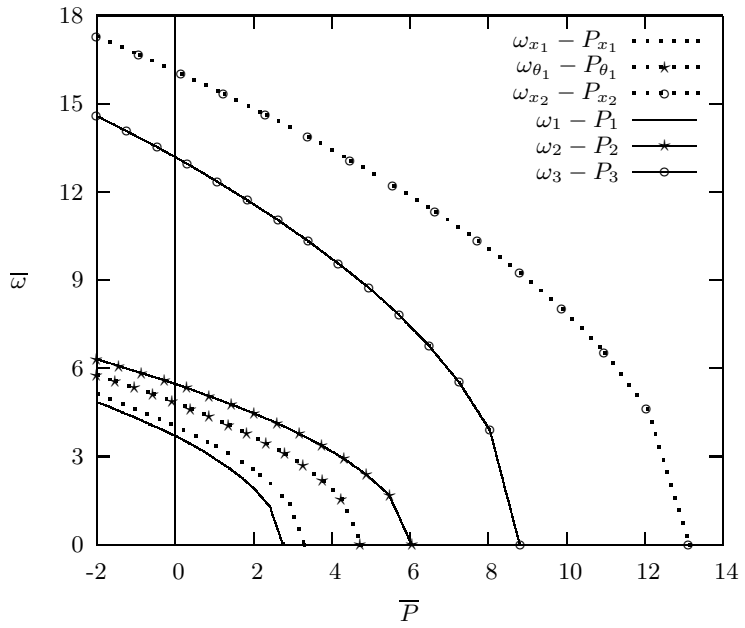

FIG. 10 Effect of axial force on the first three natural frequencies with the fiber angle 30° in the bottom flange of a simply supported composite beam.

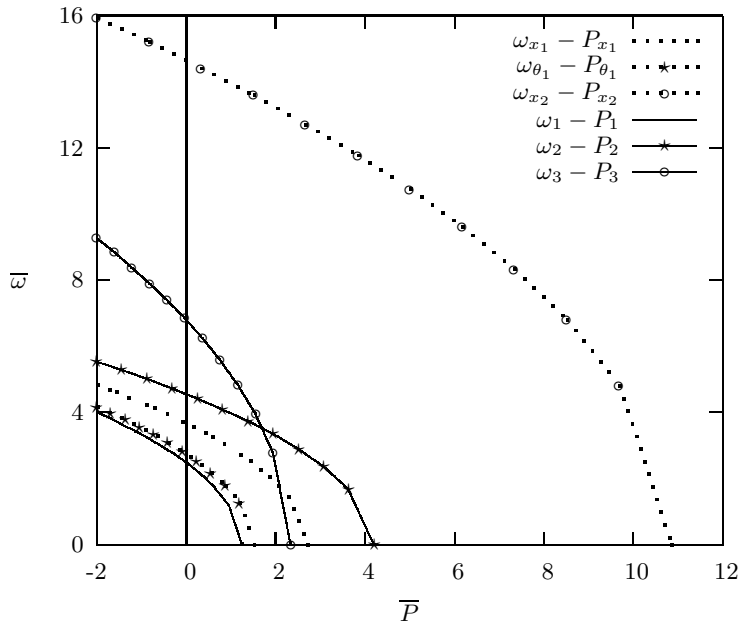

FIG. 11 Effect of axial force on the first three natural frequencies with the fiber angle 60° in the bottom flange of a simply supported composite beam.

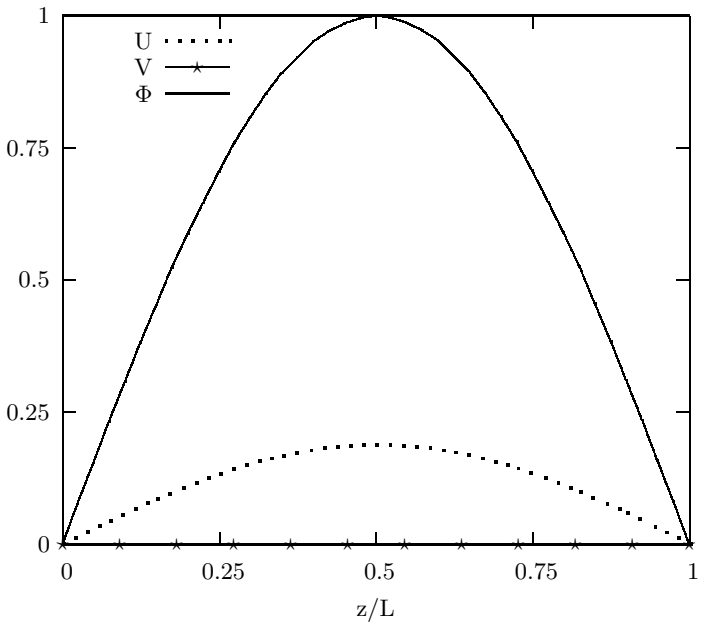

FIG. 12 Mode shapes of the flexural and torsional components for the first mode $\omega_1 = 2.615$ with the fiber angle 30° in the bottom flange of a simply supported composite beam under an axial compressive force ($\overline{P} = 0.5\overline{P}_{cr}$).

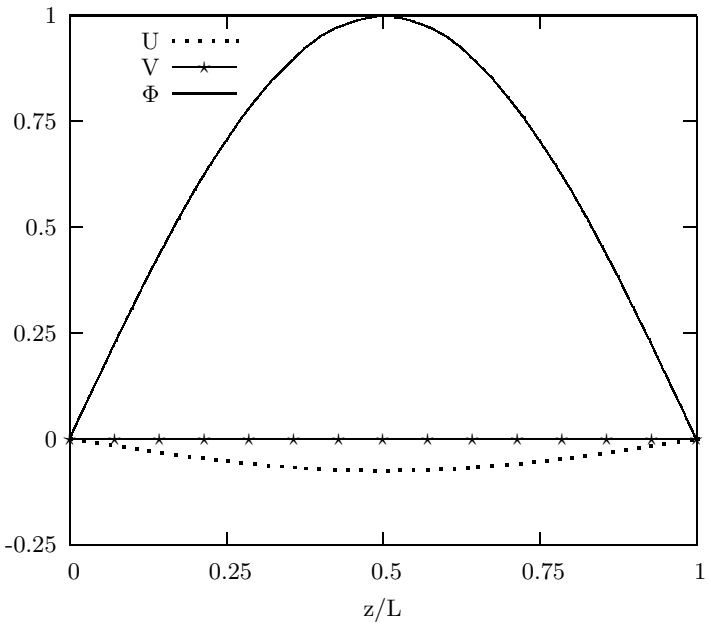

FIG. 13 Mode shapes of the flexural and torsional components for the second mode $\omega_2 = 4.805$ with the fiber angle 30° in the bottom flange of a simply supported composite beam under an axial compressive force ($\overline{P} = 0.5\overline{P}_{cr}$).

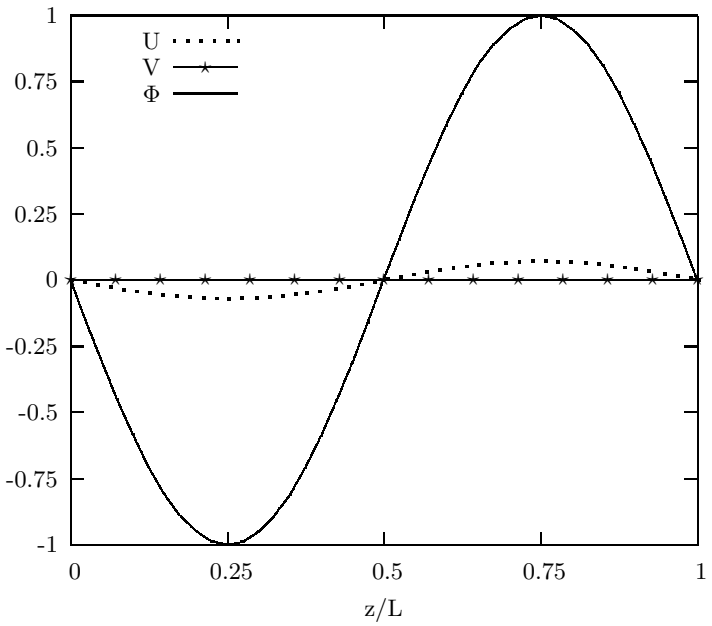

FIG. 14 Mode shapes of the flexural and torsional components for the third mode $\omega_3 = 12.107$ with the fiber angle 30° in the bottom flange of a simply supported composite beam under an axial compressive force ($\overline{P} = 0.5\overline{P}_{cr}$).

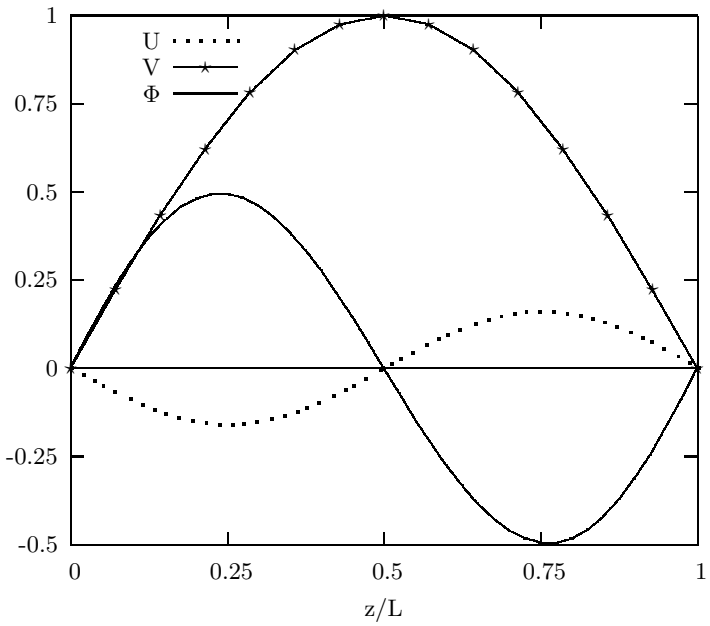

FIG. 15 Mode shapes of the flexural and torsional components for the fourth mode $\omega_4 = 16.221$ with the fiber angle 30° in the bottom flange of a simply supported composite beam under an axial compressive force ($\overline{P} = 0.5\overline{P}_{cr}$).

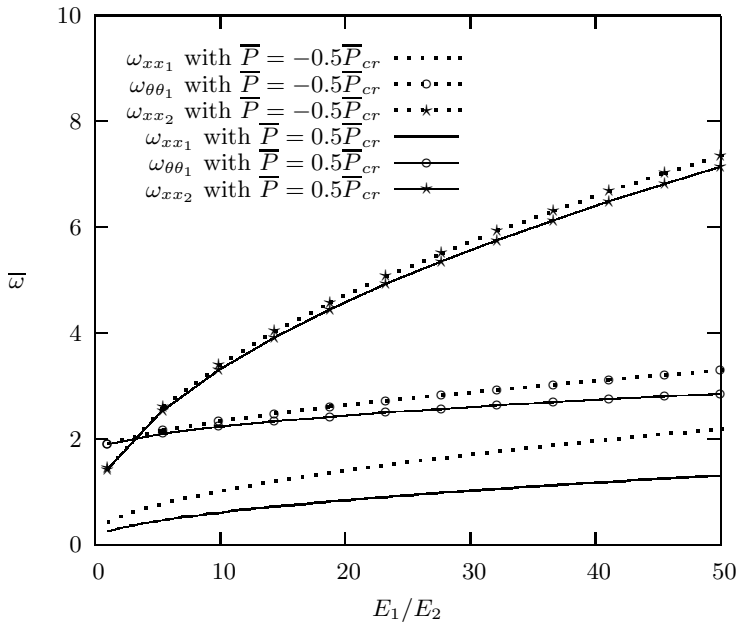

FIG. 16 Variation of the first three natural frequencies with respect to modulus ratio change of a cantilever composite beam under an axial compressive force ($\overline{P} = 0.5\overline{P}_{cr}$) and tensile force ($\overline{P} = -0.5\overline{P}_{cr}$).